EFFECTS OF PARTIAL OXIDATION OF PMAN CARBON ON THEIR PERFORMANCE AS ANODES IN 1M $LiPF_6$/EC-DMC SOLUTIONS

Ronald A. Guidotti
Battery Development Dept., P.O. Box 5800
Sandia National Laboratories
Albuquerque, NM 87185-0614

1. ABSTRACT

A study was undertaken to examine the effects of partial oxidation on the electrochemical performance of carbons derived from poly(methylacrylonitrile) (PMAN)-divinylbenzene (DVB) co-polymers. Mild oxidation was examined as a possible technique to increase the reversible capacity, improve cycleability, and reduce the amount of irreversible capacity associated with the formation of the passivation layer during the first reduction. Oxidizing conditions involved treatment of the PMAN carbon prepared at 700°C with dry CO_2 or with steam at 600°C for one hour. The effects on the performance in 1M $LiPF_6$/ethylene carbonate (EC)-dimethyl carbonate (DMC) solutions were evaluated by galvanostatic cycling tests, complex-impedance spectroscopy, and, to a more limited extent, cyclic voltammetry. Partial oxidation of PMAN carbon showed little or no overall beneficial effects in performance relative to the control.

2. INTRODUCTION

The electrochemical performance of carbon materials as anodes in Li-ion intercalation cells depends to a great extent on the bulk and surface chemistry of the material as well as a number of key physical properties, such as interplanar lattice spacing and the degree of order [1-3]. The type of solvent and supporting electrolyte also impact the electrochemical behavior, by influencing the passivation layer that forms during the first intercalation (reduction) step as well as the storage capacity for Li [4, 5]. This film is thought to be necessary for proper functioning of carbons in Li-ion cells [6].

Treatment of the carbon surface has been examined as a way of improving the electrochemical properties for use in Li-ion cells. Peled *et al.* reported that mild oxidation (6% "burnoff") of graphite by air at 550°C increased the reversible capacity and reduced the irreversible capacity [7, 8]. They attributed this improvement to formation of nanopores and the enhanced bonding of the carbon to the passivation layer through carboxylic groups. They extended this work to highly oriented pyrolytic graphite (HOPG) and found similar results [9]. The oxidation was thought to remove irregularities on the surface that contributed to the irreversible capacity but not to the reversible capacity.

Xue and Dahn performed similar oxidation studies on carbons prepared by pyrolysis of epoxies at 1,000°C [10]. At up to 10% burnoff in dry air, the reversible capacity of the carbon decreased and the irreversible capacity increased. At higher burnoff, the reversible capacity began to increase but with a large hysteresis between intercalation and deintercalation. They attributed this behavior to modification of the pore structure during the oxidation process.

DISCLAIMER

Takamura *et al.* partially oxidized carbon fibers at 700°C in flowing oxygen and found that the reversible capacity and cycleability were improved [11]. The carbons were derived from mesophase pyrolyzed at temperatures of 1,000°C to 3,100°C. They attribute the improved performance to an increase in the effective electrochemical surface area. They also reported that vacuum heating of the carbon fibers at 1,000°C was also effective in improving the performance by removing surface hydroxyl groups.

More recently, Tibbetts *et al.* reported that oxidation in air at 640°C to 760°C of vapor-grown carbon fibers (graphitized at 2,000°C) reduced the extent of electrolyte decomposition compared to the unoxidized graphite [12]. They attributed this to removal of the more-active, less-graphitic carbon atoms by oxidation and to a change in the sample morphology. Bar-Tow and Peled reported similar enhancement in the performance of natural graphite that have been partially oxidized [9].

Because of the promising results observed in a number of these studies, it was decided to investigate partial oxidation of our PMAN carbons at elevated temperatures using both CO_2 and water vapor. In addition, some carbons were exposed to a low-pressure oxygen plasma in an attempt to selectively oxidize the surface layers. Electrochemical characterization involved primarily galvanostatic cycling and complex-impedance spectroscopy.

3. EXPERIMENTAL PROCEDURES

3.1 Materials

The carbon precursor was prepared by an inverse-emulsion technique from a copolymer of PMAN and DVB as a crosslinking agent in a molar ratio of 3:1, respectively [13, 14]. The polymer precursor powder was pyrolyzed under argon at 700°C for 5 hours.

The electrolyte solution for the characterization tests was 1M $LiPF_6$ in EC/DMC (1:1 v/v), made in house [15] or purchased from Merck. The water content of the solution, as measured by Karl-Fischer titration, was <50 ppm. Li foil (Foote Mineral) was used for the counter and reference electrodes.

The powdered PMAN carbon sample (~0.8 g) was contained in an alumina boat inside a quartz tube in a tube furnace. For oxidation with CO_2, the sample was first heated under argon to 600°C. The argon was then turned off and the CO_2 was admitted into the furnace tube. The sample was oxidized under flowing CO_2 gas (~50 $cc.min^{-1}$) for one hour. The CO_2 was then shut off and the sample was cooled to ambient under flowing argon. Before entry into the furnace tube, the commercial-grade CO_2 was first passed through a drying tube filled with 4A molecular sieves. In the case of the steam oxidation, a water-saturated stream of argon (P_{H2O} ~0.03 atm) was used in place of the CO_2 under identical heating conditions. The carbon was weighed before and after the heating procedure to determine the extent of oxidation (burn off).

The treatment of the carbon with an oxygen plasma was carried using a plasma etcher (LFE Corp., Model PUC301). The PMAN carbon was placed in a quartz boat in the chamber which was then pumped out. A flow of oxygen (50 $cc.min^{-1}$) was introduced while the chamber was continually pumped. The system pressure was estimated to be <100 torr Hg. The sample was subjected to a 50-W plasma for one minute and was then stirred and subjected to a second one-minute plasma treatment.

3.2 Cells

The three-electrode system used to test the carbons has been previously described [15, 16]. The anode was made with carbon powder, 15%[1] w/o polyvinylidene fluoride (PVDF, Kynar 461) as a binder, and 5% Super 'S' carbon as a conductive additive and was pasted onto a Cu substrate using the "doctor blade" technique with dimethylformamide as the medium. After pasting, the anodes were vacuum dried for an hour at 140°-160°C. The anode discs were 1.27 cm in diameter (1.27 cm^2 area) and 0.007 to 0.021 cm thick. The anode was separated from the 0.025-cm-thick Li counter electrode by two Celgard 2500 separators. A Li flag was used as a reference electrode. The mass of active carbon ranged from 2 mg to 6 mg. Cell assembly was conducted in a dry room maintained at a dew point of less than -60°C. The cells were evacuated and backfilled with electrolyte solution in a glove box where the moisture and oxygen content were <10 ppm each. After filling, the cells were allowed to stand overnight at open circuit (OC) before testing.

3.3 Apparatus

Galvanostatic testing of the cells was performed using an Arbin Corp. Battery Test System. The test profile consisted of cycling at 0.50 $mA.cm^{-2}$ between 2 V and 0.01 V for 20 cycles. (This corresponded to an average rate of $C.1^{-1}$ to $C.3^{-1}$.) An open-circuit wait of 600 s was imposed between charge and discharge. Most of the cells were then subjected to an additional 12 cycles at rates of 0.25 $mA.cm^{-2}$ to 4 $mA.cm^{-2}$, to obtain rate-capability information.

Complex-impedance measurements were performed using a Solartron Model 1250 Frequency Response Analyzer coupled to a Solartron Model 1286 Electrochemical Interface. The impedance spectra were normally taken over a frequency range of 65 kHz to 100 mHz. Complex-impedance spectra of the carbon samples during galvanostatic cycling were taken at open circuit before intercalation and at 2 V, 0.5 V, and 0.01 V during the first intercalation. Similar measurements were taken at 2 V, at the end of one complete intercalation/deintercalation cycle. The current was allowed to decay to <50 μA at each of the measurement potentials before the cell was removed for impedance testing.

Cyclic voltammograms (CVs) were generated using a Princeton Applied Research Model 263 potentiostat. The cell was scanned between voltage limits of 3 V and 0.01 V at a sweep rate of 1 $mV.s^{-1}$.

4. RESULTS

4.1 Galvanostatic Cycling

The results of the galvanostatic cycling at 0.5 $mA.cm^{-2}$ are summarized in Table I for the first and 20th cycles. The load capacity refers to intercalation of Li^+, while unloading refers to deintercalation of Li^+. Q_{irr} is the irreversible capacity loss during the first cycle. Fade is defined as the loss of capacity per cycle between the 11th and 20th cycle. Each test was generally repeated at least twice. The typical range of composition for the PMAN carbons pyrolyzed at 700°C was: 86.61%-89.91% C, 3.58%-3.61% N, 3.41%-6.12% O, and 1.04%-1.20% H. (There may also have been some sulfur present from the ammonium persulfate used to initiate the polymerization of the methylacrylonitrile precursor.)

The extent of mass loss for the CO_2-treated PMAN carbon sample was about 3.5%. At this level of oxidation (burnoff), the total capacity (loading) during the first cycle was improved over the control, but the irreversible capacity increased by 23%. Consequently, the reversible (unload) capacity and the

[1] Unless otherwise stated, all percentages are on a weight basis.

coulombic efficiency were slightly lower. By the 20th cycle, the CO_2-oxidized sample has only a slightly greater reversible capacity but exhibited greater fade. The increase in irreversible capacity at a burnoff level of 3.5% is similar to what Dahn reported for carbons derived from epoxies for burnoff levels up to 10% in air.

The extent of mass loss for the H_2O-treated PMAN carbon sample was about 7.1%, or twice that of the CO_2-treated PMAN carbon. At this level of oxidation, the total capacity during the first cycle was considerably less than that of the control and the coulombic efficiency was also less. However, the irreversible capacity was comparable. By the 20th cycle, the reversible capacity of the H_2O-treated PMAN carbon was still less than that for the control and the efficiency remained lower as wel. It was below that of the CO_2-treated PMAN carbon as well. The fade was slightly lower, however. Overall, treatment with steam was detrimental to the electrochemical performance of the PMAN carbon for both the first cycle and with subsequent cycling. Treatment with CO_2, on the other hand, was more detrimental during the first cycle, with little benefit on the cycleability.

Relative to the control, treatment of PMAN carbon with an O_2 plasma increased the total capacity during the first cycle by a third, but at the expense of a 25% increase in the irreversible capacity. The reversible capacity on the first cycle was still about 25% greater after the treatment relative to the control. After 20 cycles, the reversible capacity was still about 37% greater than that of the control and the coulombic efficiency was comparable.

The effects of rate on the reversible capacities of the various PMAN carbons are shown in Figure 1 Corresponding data at rates other than 0.5 $mA.cm^{-2}$ were not available for the control PMAN carbon. However, comparable data for a sister lot of material were available and are included for comparison. The reversible capacity was improved for the CO_2-treated PMAN over the untreated carbon up to ~2 $mA.cm^{-2}$. The reversible capacities for the H_2O-treated PMAN were slightly lower than those for the control. The loss in capacity with increasing rate was similar for the CO_2-treated and H_2O-treated PMAN carbons and was slightly greater than that for the control. (No data were available for the O_2-plasma-treated sample at a rate other than 0.5 $mA.cm^{-2}$.)

The derivative of the capacity-voltage trace from galvanostatic cycling experiments can provide useful information on electrode processes. Figures 2 to 5 show the dC/dV-V data for the first two cycles for galvanostatic cycling at 0.5 $mA.cm^{-2}$, for the control PMAN, the CO_2-treated sample, the H_2O-treated sample, and the sample exposed to the O_2-plasma, respectively. During the first intercalation cycle, a sharp reduction peak was observed for the control sample at 1.09 V with a weaker peak at 0.77 V vs. Li/Li^+ (Fig. 2). There was also a broad oxidation wave at 1.18 V. The reduction peaks are associated with formation of the passivation layer and disappeared on the second cycle. The oxidation peak is most likely associated with Li intercalation, since it was still present during the second cycle.

The dC/dV-V plot for the CO_2-treated carbon (Fig. 3) showed two main reduction peaks at 0.94 V and 0.69 V during the first cycle. However, there was also a weak reduction peak at 1.46 V that was not observed for the control. The peak at 0.69 V was more pronounced than the one at 0.94 V. As for the control, the reduction peaks disappeared on the second cycle but the broad oxidation peak at 1.19 V remained.

The dC/dV-V plot for the H_2O-treated carbon (Fig. 4) showed a weak reduction peak at 1.31 V [similar to the peak at 1.46 V for the CO_2-treated carbon (Fig. 3)] and a major broad reduction peak at 0.72 V during the first cycle. A broad oxidation peak also occurred at 1.18 V that remained during the second cycle where the previous reduction peaks were no longer observed.

The dC/dV-V plot for the O_2-plasma-treated carbon (Fig. 5) showed two broad reduction peaks at 0.93 V and 0.63 V during the first cycle, the latter being similar to the peak at 0.72 V for the H_2O-treated carbon (Fig. 4). Again, a reversible, broad oxidation peak occurred at 1.15 V.

The derivative plots show distinctive signatures that reflect differences in treatment of the PMAN carbons. During the first intercalation, all carbons showed peaks associated with irreversible reduction processes. They may involve the solvent or electrolyte or possibly oxygenated functional groups on the carbon surface. Likewise, all showed a broad reversible oxidation peak most likely associated with the intercalation process. However, it should be noted that the derivative data from galvanostatic cycling experiments are not equivalent to a cyclic voltammogram, as the latter is voltage controlled while the former is current controlled. The derivative data will therefore not provide the same oxidation and reduction peaks as observed in cyclic voltammograms. This is evident in Figure 6 for a CV for a representative 700°C PMAN carbon taken at a scan rate of 1 $mV.s^{-1}$ between 3 V and 0.01 V.

The CV for the first cycle showed a broad reduction peak at 1.14 V and two sharper reduction peaks at 0.84 V and 0.56 V. There was also a broad oxidation peak during the first cycle at 1.10 V. This peak was still present during the second and third cycles which indicates association with a reversible process, such as intercalation or a reversible redox reaction (*e.g.*, quinone-hydroquinone). Except for the broad peak at 1.14 V, these reduction peaks are related to irreversible processes involving passive film formation and diminish during the second cycle and disappear by the third cycle. Qualitatively, there is reasonably good agreement with the nature of the electrode processes that are indicated by the CVs and the derivative data.

4.2 Complex Impedance

Figure 7 shows the complex-impedance spectra before intercalation for the PMAN carbon before (control) and after various oxidative treatments. All the treated samples showed a capacitive response similar to that of a porous-electrode; this was not evident for the control sample. The corresponding spectra for the first reduction to a potential of 0.01 V are shown in Figure 8. All the spectra exhibited an inductive loop, with the H_2O-treated sample having the least inductance.

This low-frequency inductive behavior is typical of what we have observed for many disordered carbons in 1M $LiPF_6$/EC-DMC electrolyte during the first reduction cycle at potentials of 0.5 V or less. This has been reported previously for our PMAN carbons [15, 16]. Processes involving Li plating can be dismissed, as they would be observed for every cycle. It is believed that this inductive behavior is related to the formation of intermediate moieties as part of the formation of the passivation layer on the high-surface-area (32 $m^2.g^{-1}$) PMAN carbon through unknown solvent/electrolyte reduction processes. The inductive loop disappears completely after four to five cycles, when the majority of the passive-film formation has occurred. At this point the impedance spectrum then shows two semicircles and a Warburg tail [15]. [The first (high-frequency) semicircle is associated with charge transfer at the film-carbon interface and the second (low-frequency) semicircle is associate with intercalation into the carbon. The Warburg tail is associated with Li^+ diffusion through the passive film on the carbon.] Similar inductive behavior has been reported during electrodeposition of Ni from H_2SO_4 solutions [17-20]. A strong inductive component related to film formation was also observed for the Ca anode in $Li/SOCl_2$ cells [21].

Figure 9 shows complex-impedance spectra of the various PMAN carbons at 2 V OC after one complete intercalation/deintercalation cycle. The spectra now exhibited a small, depressed, high-frequency semicircle (not evident at the scale used in the plot) with a pseudo-Warburg tail. The diameters of the semicircles were <15 ohms which is consistent with reasonably facile reaction kinetics for this type of

carbon. The angle of the tail ranged from 70° for the control and 52° to 60° for the treated samples. These angles are greater than the ideal value of 45° for a purely diffusion process.

5. DISCUSSION

The various oxidizing agents involve different chemistries with corresponding differences in thermodynamics, as illustrated by the following chemical reactions at 600°C:

CO_2 Treatment: (1)	$CO_2 + C \text{ ----> } 2CO$	($\Delta G^\circ = +17.67$ kJ.mol^{-1})	
H_2O Treatment:	$H_2O + C \text{ ----> } CO + H_2$	($\Delta G^\circ = +10.6$ kJ.mol^{-1})	(2)
O_2 Treatment:	$O_2 + C \text{ ----> } CO_2$	($\Delta G^\circ = -395.7$ kJ.mol^{-1})	(3a)
	$0.5O_2 + C \text{ ----> } CO$	($\Delta G^\circ = -189.0$ kJ.mol^{-1})	(3b)

Treatment with O_2 is by far the most thermodynamically favorable at 600°C, for both CO and CO_2 reaction products (eqn. 3a and 3b, respectively). In contrast, CO_2 treatment is the least thermodynamically favorable at 600°C (eqn. 1), with ΔG° becoming negative near 700°C. Treatment with H_2O at 600°C (eqn. 2) is somewhat more thermodynamically favorable than treatment with CO_2 (eqn. 2). ΔG° becomes negative near 670°C. Nevertheless, the kinetics for oxidation of the carbon with CO_2 and H_2O were adequate at 600°C to provide mass loss of carbon of 3.5% and 7.1%, respectively, after one hour. The equilibrium was driven sufficiently to the right under the steady-state conditions that existed during the carbon heat treatments under a flowing-gas regime to provide adequate removal of material. The kinetics would be even faster for oxidation with O_2 or air.

Because of the different chemistries involved, the effects on the carbon of these various oxidative treatments may not lead to comparable results, even though carbon is consumed in all cases. There could be distinct differences in morphology and in the resulting pore structure during carbon removal as CO or CO_2. This, in turn, could have a measurable impact on the electrochemical performance by affecting the true electrochemical surface area available, which can be much less than that obtained by the classical BET nitrogen-adsorption method. Pores that are microscopic (nanopores), for example, can prevent access of electrolyte for redox reactions.

5. CONCLUSIONS

The effect of partial oxidation of PMAN carbons on its electrochemical performance in 1M $LiPF_6$/EC-DMC (1:1 v/v) was studied. Oxidation in a stream of CO_2 at a burnoff of 3.5% has little overall beneficial effect on performance. While the total capacity is increased slightly (~9%) during the first cycle, the irreversible capacity increases by almost a fourth. This is in agreement with results reported by Xue and Dahn for air-oxidation of their disordered carbons derived from epoxies [10]. There is slight improvement in the reversible capacity (~7%) by the 20th cycle, but there is also a slight drop in the coulombic efficiency relative to the control. At rates between 0.25 and ~2 mA.cm^{-2}, the CO_2 -treated carbon shows a slight improvement in the reversible capacity over the control.

Steam oxidation of PMAN carbon does not result in improvement in its electrochemical performance. Oxidation of PMAN carbon in a stream of H_2O-saturated argon (P_{H2O} ~3 atm) to a burnoff of 7.1%

reduces the total capacity relative to the control but the irreversible capacity remains essentially unchanged. By the 20th cycle, the reversible capacity remains less than for the control and the coulombic efficiency is lower–below that of the CO_2-treated PMAN carbon. The rate capability of the stream-treated carbon is inferior to that of the control.

Treatment of the PMAN carbon in an oxygen plasma yields the highest total capacity but also the highest irreversible capacity of all the oxidative processes examined. The reversible capacity is improved on the first cycle and remains higher than the control at the 20th cycle. The fade and coulombic efficiencies are comparable. The high irreversible capacities resulting from the treatment with an oxygen plasma make this process unattractive, even with the improvement realized in the reversible capacity.

The derivative plots of the galvanostatic voltage-capacity traces (*i.e.*, dC/dV-V plots) are similar yet distinctive for the various treatment processes. The control shows two well-defined reduction peaks during the first reduction at 1.09 V and 0.77 V (vs. Li/Li^+) associated with passive-film formation. There is also a broad reversible oxidation peak at 1.18 V. These peaks disappear on the second cycle. Similar peaks are observed for the treated carbons but with slight shifts in the reduction potentials and broading of the peaks.

The complex-impedance spectra for the PMAN carbons change dramatically as a function of potential during the first reduction/intercalation. At OCV, the treated carbons show the typical porous-electrode response that is not present for the untreated sample. At 0.01 V, where passive-film formation is occurring along with intercalation, strong inductive behavior is observed that is believed due to the generation of intermediates involved with film formation. The steam-treated carbon shows the least inductive behavior. After one complete intercalation cycle, all the carbons are covered with a substantial passivation layer. The complex-impedance spectra then consist of a small depressed semicircle (<15 ohms in diameter) and a pseudo-Warburg tail with an angle greater than the ideal value of 45° for a purely diffusion process.

The differences in electrochemical performance of PMAN after the various oxidative treatments may be related to changes in the pore structure or morphology of the resulting products under the present test conditions. Higher levels of oxidation or higher temperatures may be beneficial to performance.

6. Acknowledgments

The authors wish to acknowledge the assistance H. Case and M. Overstreet for construction of the cells. W. Even, Jr. and M. Hunter prepared the PMAN samples and performed the experiment involving oxygen-plasma treatment.

This work was supported by the United States Department of Energy under Contract DE-AC04-94AL85000.

REFERENCES

1. O. Yamamoto, N. Imanishi, Y. Takeda, and H. Kashiwagi, *J Power Sources*, **54**, 72 (1995).
2. Y. Matsumura, S. Wang, T. Kasuh, and T. Maeda, *Syn. Met.*, **71**, 1755 (1995).
3. J. R. Dahn, A. K. Sleigh, H. Shi, B. M. Way, W. J. Weydanz, J. N. Reimers, Q. Zhong, and U. von Sachen, in *Lithium Batteries–New Materials, Development, and Perspectives*, G. Pistoia, ed., pp. 1-48, Elsevier, New York (1994).
4. C.-K. Huang, S. Surampudi, and G. Halpert, *Proc. 36th Power Sources Conf.*, 61 (1994).
5. D. Aurbach, Y. Ein-Eli, O. Chusid, Y. Carmeli, M. Babai and H. Yamin, *J. Electrochem. Soc*, **141** (3), 603 (1994).

6. E. Peled, D. Bar Tow, A. Melman, E. Gerenrot, Y. Lavi, and Y. Rosenberg, *in Proc. of the Symp. on Lithium Batteries*, **PV 94-4**, Doddapaneni and A. R. Landgrebe, eds., 177 (1994).
7. E. Peled, C. Menachem, B. Bar-Tow, and A. Melman, *J. Electrochem. Soc.*, **143** (1), L4 (1996).
8. C. Menachem, E. Peled, and L. Burstein, *Proc. 37th Power Sources Conf.*, 208 (1996).
9. D. Bar-Tow and E. Peled, *Ext. Abst.of Fall Mtg. of The Electrochem. Soc., San Antonio, TX,* **Vol. 96-2**, 1028 (1996).
10. J. S. Xue and J. R. Dahn, *J. Electrochem. Soc.*, **142** (11), 3668 (1996).
11. T. Takamura, M. Kikuchi, and Y. Ikezawa, *The Electochem. Soc. Proc.* **94-28**, 213 (1994).
12. G. C. Tibbets, G.-Abbas Narri, and B. J. Howie, *Ext. Abst.of Fall Mtg. of The Electrochem. Soc., San Antonio, TX,* **Vol. 96-2**, 117 (1996).
13. W. R. Even. and D. P. Gregory., *MRS Bull.*, **1994**, *XIX* (4), 29.
14. Delnick, F. M., W. R., Even, Jr., A. P Sylwester, J. C. F. Wang, and T. Zifer, **U.S. Patent 5,426,006**, June 20, 1995.
15. R. Guidotti and B. Johnson, *Proc. 11th Ann. Battery Conf. on Applic. and Advances*, 193 (1996).
16. R. A. Guidotti, B. J. Johnson, and W. Even, Jr., *Proc. 37th Power Sources Conf.*, 219 (1996).
17. I. Epelboin and M. Keddam, *Electrochim. Acta*, **17**, 177 (1972).
18. H. G. Feller, H. J. Ratzer-Scheibe, and W. Wendt, *Electrochim. Acta*, **17**, 187 (1972).
19. I. Epelboin, M. Jousselin, and R. Wiart, *J. Electroanal. Chem.*, **101**, 281 (1971).
20. I. Epelboin and R. Wiart, *J. Electrochem. Soc*, **118**, 1577 (1971).
21. E. Elster, R. Cohen, and E. Peled, *J. Power Sources*, **26**, 423 (1989).

TABLE I. EFFECT OF PARTIAL OXIDATION ON THE PERFORMANCE OF 700°C PMAN CARBON

	First Cycle				20th Cycle				
Oxidant	Load ($mAh.g^{-1}$)	Unload ($mAh.g^{-1}$)	Effic. (%)	Q_{irr} ($mAh.g^{-1}$)	Load ($mAh.g^{-1}$)	Unload ($mAh.g^{-1}$)	Effic. (%)	Fade ($mAh.g^{-1}cyc^{-1}$)	Comments
None (baseline)	675.6	328.7	48.6	346.8	218.8	214.9	98.2	-1.40	Std. 32 cycles
CO_2 (3.5% burnoff)	735.8	310.5	42.3	425.3	233.8	229.3	98.1	-1.73	Std. 32 cycles
H_2O (7.1% burnoff)	628.2	273.4	43.5	355.9	196.7	192.3	97.8	-1.15	Std. 32 cycles
O_2 Plasma	906.3	410.0	45.2	496.3	299.7	294.7	98.3	-1.42	Only 20 cycles

All cells were tested in 1M $LiPF_6$/EC-DMC (1:1 v/v) at room temperature between 2 V and 0.01 V at 0.5 $mA.cm^{-2}$ for either 20 or 32 cycles.

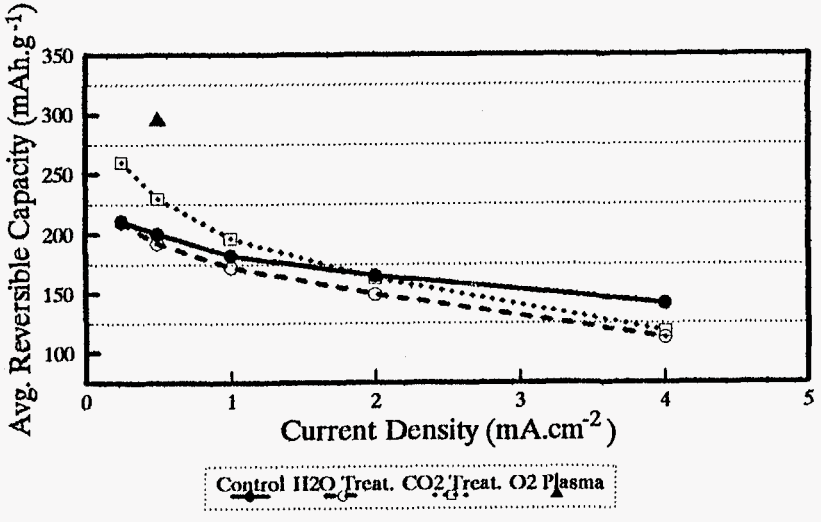

Fig. 1. PERFORMANCE OF PMAN CARBON AS A FUNCTION OF RATE FOR VARIOUS TREATMENTS.

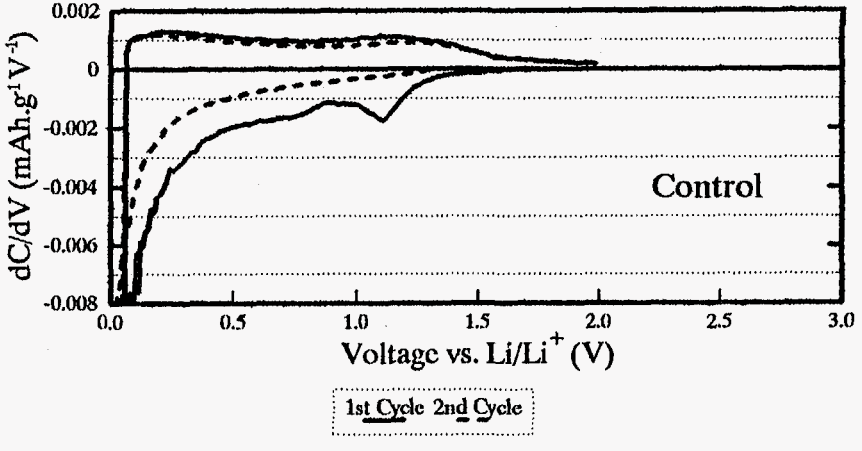

Fig. 2. DERIVATIVE OF CAPACITY-VOLTAGE PLOT VS. VOLTAGE FOR CONTROL PMAN CARBON IN 1M/$LiPF_6$/EC-DMC SOLUTION.

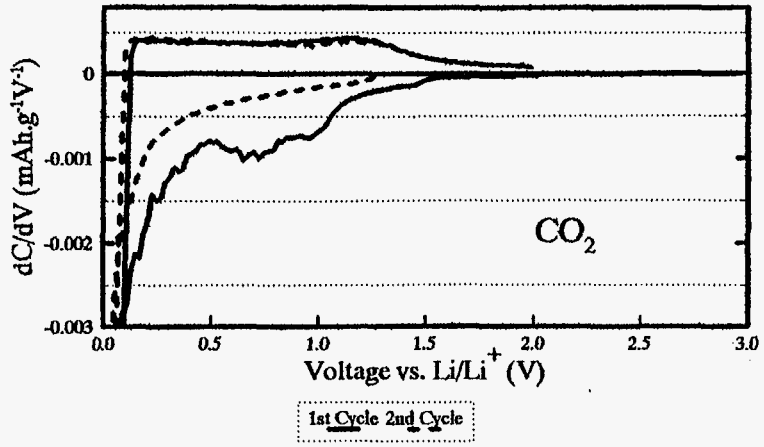

Fig. 3. DERIVATIVE OF CAPACITY-VOLTAGE PLOT VS. VOLTAGE FOR CO_2-TREATED PMAN CARBON IN 1M/$LiPF_6$/EC-DMC SOLUTION.

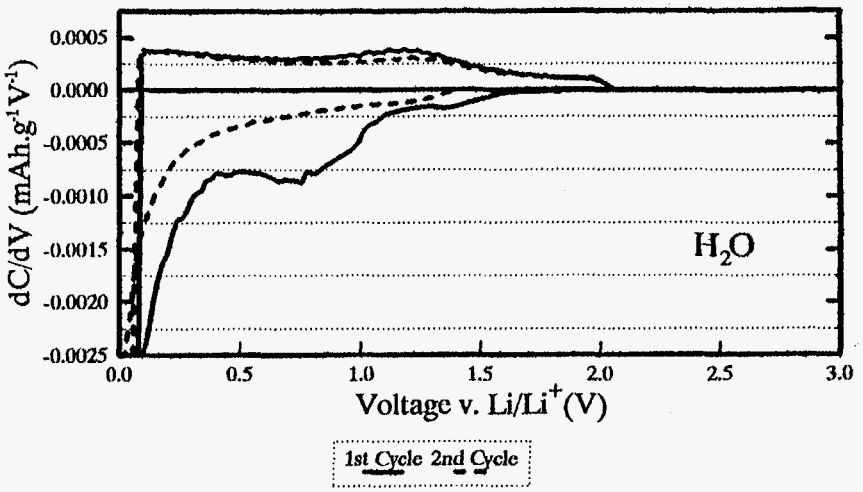

Fig. 4. DERIVATIVE OF CAPACITY-VOLTAGE PLOT VS. VOLTAGE FOR H_2O-TREATED PMAN CARBON IN 1M/$LiPF_6$/EC-DMC SOLUTION.

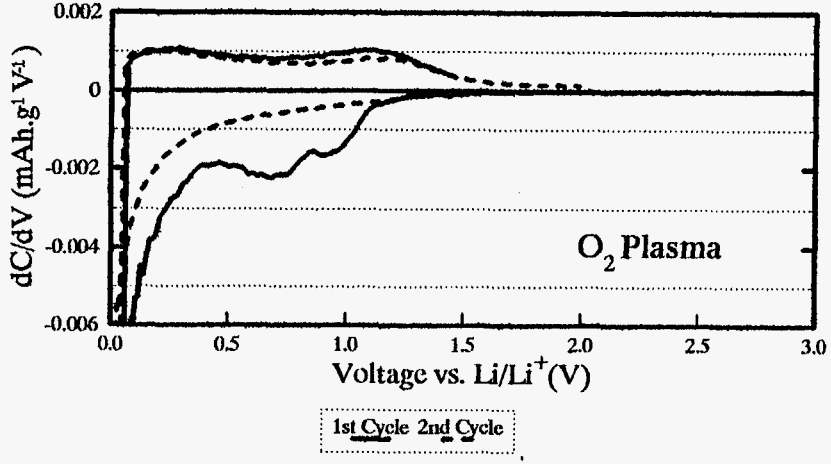

Fig. 5. DERIVATIVE OF CAPACITY-VOLTAGE PLOT VS. VOLTAGE FOR O_2-PLASMA-TREATED PMAN CARBON IN 1M/$LiPF_6$/EC-DMC SOLUTION.

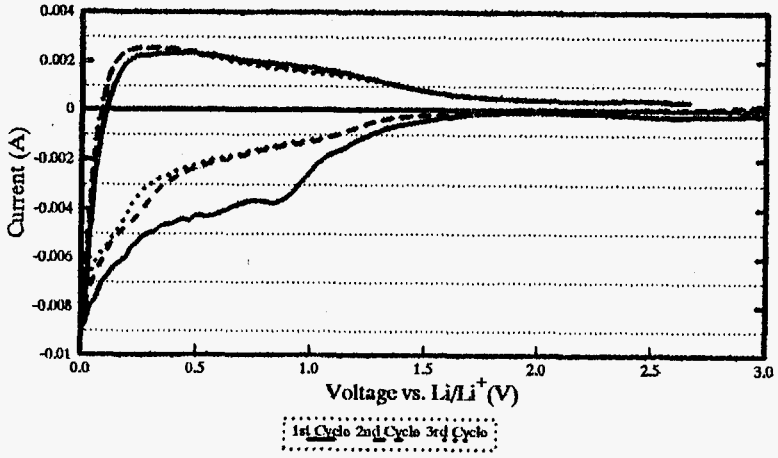

Fig. 6. CYCLIC VOLTAMMOGRAMS OF PMAN CARBON IN 1M/$LiPF_6$/EC-DMC. SCAN RATE = 1 $mV.S^{-1}$.

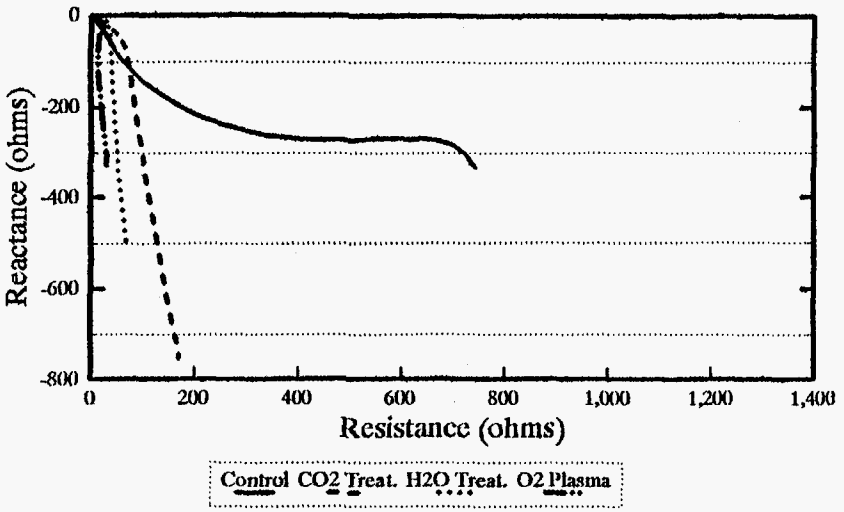

Fig. 7. COMPLEX IMPEDANCE SPECTRA PRIOR TO INTERCALATION IN 1M/$LiPF_6$/EC-DMC OF PMAN CARBON FOR VARIOUS TREATMENTS.

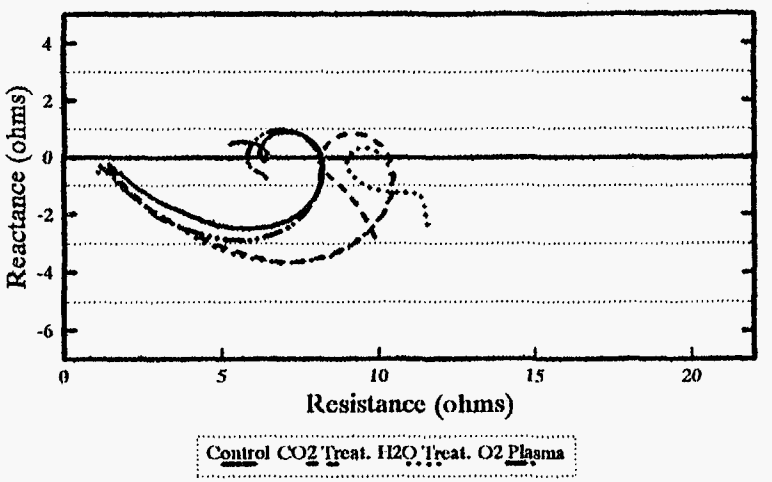

Fig. 8. COMPLEX IMPEDANCE SPECTRA AT O.O1 V DURING FIRST INTERCALATION IN 1M/$LiPF_6$/EC-DMC OF PMAN CARBON FOR VARIOUS TREATMENTS.

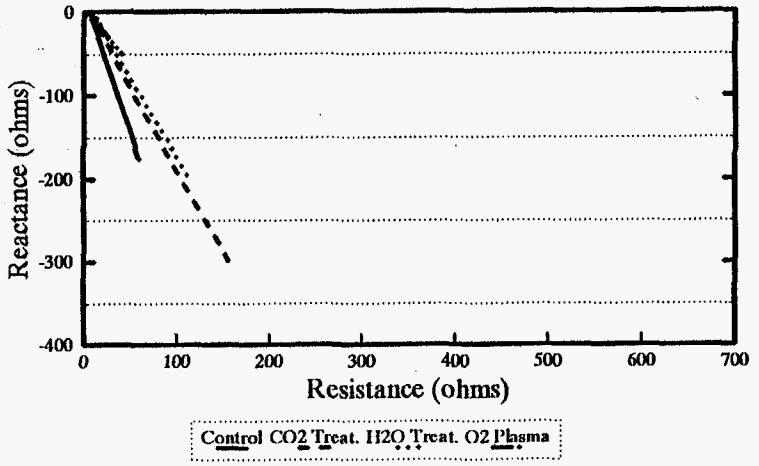

Fig. 9. COMPLEX IMPEDANCE SPECTRA AT 2 V AFTER ONE COMPLETE INTERCALATION/DEINTER-CALATION IN 1M/$LiPF_6$/EC-DMC OF PMAN CARBON.